

Study of the suppressed B meson decay $B^- \rightarrow DK^-, D \rightarrow K^+\pi^-$

Y. Horii,⁴¹ K. Trabelsi,⁸ H. Yamamoto,⁴¹ I. Adachi,⁸ H. Aihara,⁴² K. Arinstein,¹ V. Aulchenko,¹ V. Balagura,¹³ E. Barberio,²¹ I. Bedny,¹ K. Belous,¹² V. Bhardwaj,³³ U. Bitenc,¹⁴ S. Blyth,²⁵ A. Bozek,²⁷ M. Bračko,^{20,14} T. E. Browder,⁷ Y. Chao,²⁶ A. Chen,²⁴ W. T. Chen,²⁴ B. G. Cheon,⁶ R. Chistov,¹³ I.-S. Cho,⁴⁷ S.-K. Choi,⁵ Y. Choi,³⁷ J. Dalseno,⁸ M. Dash,⁴⁶ S. Eidelman,¹ N. Gabyshev,¹ H. Ha,¹⁶ J. Haba,⁸ T. Hara,³² K. Hayasaka,²² M. Hazumi,⁸ D. Heffernan,³² Y. Hoshi,⁴⁰ W.-S. Hou,²⁶ H. J. Hyun,¹⁷ K. Inami,²² A. Ishikawa,³⁴ H. Ishino,⁴³ R. Itoh,⁸ M. Iwabuchi,⁴ M. Iwasaki,⁴² Y. Iwasaki,⁸ D. H. Kah,¹⁷ H. Kajji,²² J. H. Kang,⁴⁷ N. Katayama,⁸ H. Kawai,² T. Kawasaki,²⁹ H. Kichimi,⁸ H. J. Kim,¹⁷ S. K. Kim,³⁶ Y. J. Kim,⁴ K. Kinoshita,³ S. Korpar,^{20,14} P. Križan,^{19,14} P. Krokovny,⁸ C. C. Kuo,²⁴ Y. Kuroki,³² A. Kuzmin,¹ Y.-J. Kwon,⁴⁷ J. S. Lee,³⁷ M. J. Lee,³⁶ S. E. Lee,³⁶ T. Lesiak,²⁷ J. Li,⁷ S.-W. Lin,²⁶ C. Liu,³⁵ D. Liventsev,¹³ F. Mandl,¹¹ S. McOnie,³⁸ T. Medvedeva,¹³ W. Mitaroff,¹¹ K. Miyabayashi,²³ H. Miyake,³² H. Miyata,²⁹ Y. Miyazaki,²² R. Mizuk,¹³ G. R. Moloney,²¹ T. Nagamine,⁴¹ Y. Nagasaka,⁹ M. Nakao,⁸ H. Nakazawa,²⁴ Z. Natkaniec,²⁷ S. Nishida,⁸ O. Nitoh,⁴⁵ S. Ogawa,³⁹ T. Ohshima,²² S. Okuno,¹⁵ H. Ozaki,⁸ G. Pakhlova,¹³ C. W. Park,³⁷ H. Park,¹⁷ H. K. Park,¹⁷ L. S. Peak,³⁸ R. Pestotnik,¹⁴ L. E. Pilonen,⁴⁶ H. Sahoo,⁷ Y. Sakai,⁸ O. Schneider,¹⁸ C. Schwanda,¹¹ A. J. Schwartz,³ K. Senyo,²² M. E. Sevior,²¹ M. Shapkin,¹² H. Shibuya,³⁹ J.-G. Shiu,²⁶ A. Somov,³ S. Stanič,³⁰ M. Starič,¹⁴ T. Sumiyoshi,⁴⁴ S. Suzuki,³⁴ F. Takasaki,⁸ N. Tamura,²⁹ M. Tanaka,⁸ Y. Teramoto,³¹ T. Tsuboyama,⁸ S. Uehara,⁸ Y. Unno,⁶ S. Uno,⁸ P. Urquijo,²¹ Y. Usov,¹ G. Varner,⁷ K. E. Varvell,³⁸ K. Vervink,¹⁸ C. H. Wang,²⁵ M.-Z. Wang,²⁶ P. Wang,¹⁰ X. L. Wang,¹⁰ Y. Watanabe,¹⁵ R. Wedd,²¹ E. Won,¹⁶ Y. Yamashita,²⁸ M. Yamauchi,⁸ C. C. Zhang,¹⁰ Z. P. Zhang,³⁵ V. Zhilich,¹ V. Zhulanov,¹ A. Zupanc,¹⁴ and O. Zykova¹

(The Belle Collaboration)

¹*Budker Institute of Nuclear Physics, Novosibirsk*

²*Chiba University, Chiba*

³*University of Cincinnati, Cincinnati, Ohio 45221*

⁴*The Graduate University for Advanced Studies, Hayama*

⁵*Gyeongsang National University, Chinju*

⁶*Hanyang University, Seoul*

⁷*University of Hawaii, Honolulu, Hawaii 96822*

⁸*High Energy Accelerator Research Organization (KEK), Tsukuba*

⁹*Hiroshima Institute of Technology, Hiroshima*

¹⁰*Institute of High Energy Physics, Chinese Academy of Sciences, Beijing*

¹¹*Institute of High Energy Physics, Vienna*

¹²*Institute of High Energy Physics, Protvino*

¹³*Institute for Theoretical and Experimental Physics, Moscow*

¹⁴*J. Stefan Institute, Ljubljana*

¹⁵*Kanagawa University, Yokohama*

¹⁶*Korea University, Seoul*

¹⁷*Kyungpook National University, Taegu*

¹⁸*École Polytechnique Fédérale de Lausanne (EPFL), Lausanne*

¹⁹*Faculty of Mathematics and Physics, University of Ljubljana, Ljubljana*

²⁰*University of Maribor, Maribor*

²¹*University of Melbourne, School of Physics, Victoria 3010*

²²*Nagoya University, Nagoya*

²³*Nara Women's University, Nara*

²⁴*National Central University, Chung-li*

²⁵*National United University, Miao Li*

²⁶*Department of Physics, National Taiwan University, Taipei*

²⁷*H. Niewodniczanski Institute of Nuclear Physics, Krakow*

²⁸*Nippon Dental University, Niigata*

²⁹*Niigata University, Niigata*

³⁰*University of Nova Gorica, Nova Gorica*

³¹*Osaka City University, Osaka*

³²*Osaka University, Osaka*

³³*Panjab University, Chandigarh*

³⁴*Saga University, Saga*

³⁵University of Science and Technology of China, Hefei

³⁶Seoul National University, Seoul

³⁷Sungkyunkwan University, Suwon

³⁸University of Sydney, Sydney, New South Wales

³⁹Toho University, Funabashi

⁴⁰Tohoku Gakuin University, Tagajo

⁴¹Tohoku University, Sendai

⁴²Department of Physics, University of Tokyo, Tokyo

⁴³Tokyo Institute of Technology, Tokyo

⁴⁴Tokyo Metropolitan University, Tokyo

⁴⁵Tokyo University of Agriculture and Technology, Tokyo

⁴⁶Virginia Polytechnic Institute and State University, Blacksburg, Virginia 24061

⁴⁷Yonsei University, Seoul

We report a study of the suppressed B meson decay $B^- \rightarrow DK^-$ followed by $D \rightarrow K^+\pi^-$, where D indicates a D^0 or \bar{D}^0 state. The two decay paths interfere and provide information on the CP -violating angle ϕ_3 . We use a data sample containing 657×10^6 $B\bar{B}$ pairs recorded at the $\Upsilon(4S)$ resonance with the Belle detector at the KEKB asymmetric-energy e^+e^- storage ring. We do not find significant evidence for the mode $B^- \rightarrow DK^-, D \rightarrow K^+\pi^-$, and set an upper limit of $r_B < 0.19$, where r_B is the magnitude of the ratio of amplitudes $|A(B^- \rightarrow \bar{D}^0 K^-)/A(B^- \rightarrow D^0 K^-)|$. The decay $B^- \rightarrow D\pi^-, D \rightarrow K^+\pi^-$ is also analyzed as a reference, for which we observe a signal with 6.6σ significance, and measure the charge asymmetry $\mathcal{A}_{D\pi}$ to be $-0.02^{+0.15}_{-0.16}(\text{stat}) \pm 0.04(\text{syst})$. In addition, the ratio $\mathcal{B}(B^- \rightarrow D^0 K^-)/\mathcal{B}(B^- \rightarrow D^0 \pi^-)$ is measured to be $[6.77 \pm 0.23(\text{stat}) \pm 0.30(\text{syst})] \times 10^{-2}$.

PACS numbers: 11.30.Er, 12.15.Hh, 13.25.Hw, 14.40.Nd

Precise measurements of the parameters of the standard model are fundamentally important and may reveal new physics. The Cabibbo-Kobayashi-Maskawa matrix [1, 2] consists of weak interaction parameters for the quark sector, one of which is the CP -violating angle $\phi_3 \equiv \arg(-V_{ud}V_{ub}^*/V_{cd}V_{cb}^*)$. Several proposed methods for measuring ϕ_3 exploit the interference between $B^- \rightarrow D^0 K^-$ and $B^- \rightarrow \bar{D}^0 K^-$, where D^0 and \bar{D}^0 decay to common final states [3, 4]. The effects of CP violation could be enhanced if the final state is chosen so that the interfering amplitudes have comparable magnitudes [5]. The decay $B^- \rightarrow DK^-, D \rightarrow K^+\pi^-$ ($D = D^0$ or \bar{D}^0) is a particularly useful mode, in which the color-favored B decay followed by the doubly Cabibbo-suppressed D decay interferes with the color-suppressed B decay followed by the Cabibbo-favored D decay (Fig. 1). Previous studies of this decay mode have not found a significant signal yield [6, 7]. The decay $B^- \rightarrow D\pi^-, D \rightarrow K^+\pi^-$ has a similar event topology and is Cabibbo-enhanced relative to the corresponding DK^- mode. Therefore this mode is an ideal control sample, while its CP asymmetry is expected to be negligible.

In this analysis, we measure the ratios of the above suppressed decays relative to the favored decays $B^- \rightarrow Dh^-, D \rightarrow K^-\pi^+$, where $h = K$ or π . The same selection criteria are used for the suppressed decays and the favored decays whenever possible in order to cancel systematic uncertainties. In this paper, charge conjugate reactions are implied except where otherwise mentioned; we denote the suppressed decays $B^- \rightarrow Dh^-, D \rightarrow K^+\pi^-$ as $B^- \rightarrow D_{\text{sup}}h^-$, and the favored decays $B^- \rightarrow Dh^-, D \rightarrow K^-\pi^+$ as $B^- \rightarrow D_{\text{fav}}h^-$. Furthermore, a K^- or π^- that originates directly from a B^- is referred to as

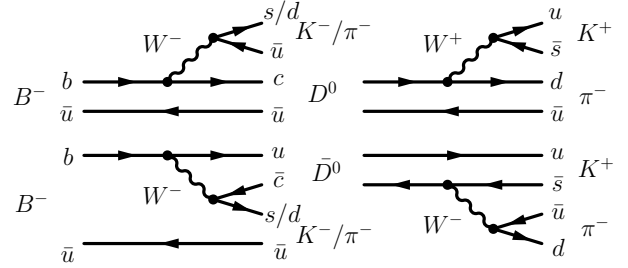


FIG. 1: Diagrams for $B^- \rightarrow DK^-, D \rightarrow K^+\pi^-$ and $B^- \rightarrow D\pi^-, D \rightarrow K^+\pi^-$ decays.

the "prompt" particle.

The results are based on a data sample that contains 657×10^6 $B\bar{B}$ pairs, collected with the Belle detector at the KEKB asymmetric-energy e^+e^- (3.5 GeV on 8 GeV) collider [8] operating at the $\Upsilon(4S)$ resonance.

The Belle detector is a large-solid-angle magnetic spectrometer that consists of a silicon vertex detector (SVD), a 50-layer central drift chamber (CDC), an array of aerogel threshold Cherenkov counters (ACC), a barrel-like arrangement of time-of-flight scintillation counters (TOF), and an electromagnetic calorimeter comprised of CsI(Tl) crystals (ECL) located inside a superconducting solenoid coil that provides a 1.5 T magnetic field. An iron flux return located outside of the coil is instrumented to detect K_L^0 mesons and to identify muons (KLM). The detector is described in detail elsewhere [9]. Two inner detector configurations were used. A 2.0 cm beam pipe and a 3-layer silicon vertex detector were used for the first sample of $152 \times 10^6 B\bar{B}$ pairs, while a 1.5 cm beam pipe, a 4-layer silicon detector, and a small-cell inner drift chamber were

used to record the remaining $505 \times 10^6 B\bar{B}$ pairs [10].

Neutral D meson candidates are reconstructed from pairs of oppositely charged tracks. For each track, we apply a particle identification requirement based on a K/π likelihood ratio $P(K/\pi) = \mathcal{L}_K/(\mathcal{L}_K + \mathcal{L}_\pi)$, where \mathcal{L}_K and \mathcal{L}_π are kaon and pion likelihoods, respectively. The likelihoods are determined by the information from the ACC and TOF and specific ionization measurements from the CDC. We use the requirements $P(K/\pi) > 0.4$ and $P(K/\pi) < 0.7$ for the kaon and pion candidates, respectively. The efficiency to identify a kaon (pion) is 94%, while the probability that a pion (kaon) is misidentified as a kaon (pion) is about 10%. The systematic error in the K/π selection efficiency is less than 1% for both kaons and pions. The invariant mass of the $K\pi$ pair must be within $\pm 3\sigma$ of the nominal D mass [11]: $1.850 \text{ GeV}/c^2 < M(K\pi) < 1.880 \text{ GeV}/c^2$. To improve the momentum determinations, tracks from the D candidate are refitted with their invariant mass constrained to the nominal D mass.

B meson candidates are reconstructed by combining a D candidate with a prompt charged hadron candidate, for which the particle identification requirement $P(K/\pi) > 0.6$ [$P(K/\pi) < 0.2$] is used for $B^- \rightarrow DK^-$ ($B^- \rightarrow D\pi^-$). With this requirement, the efficiency to identify a kaon (pion) is 86% (81%), while the probability that a pion (kaon) is misidentified as a kaon (pion) is about 5% (10%). The signal is identified by two kinematic variables, the energy difference $\Delta E = E_D + E_h - E_{\text{beam}}$ and the beam-energy-constrained mass $M_{\text{bc}} = \sqrt{E_{\text{beam}}^2 - |\vec{p}_D + \vec{p}_h|^2}$, where E_{beam} is the beam energy in the $\Upsilon(4S)$ center-of-mass (c.m.) frame. We require M_{bc} to be within $\pm 3\sigma$ of the nominal B mass [11]; namely, $5.271 \text{ GeV}/c^2 < M_{\text{bc}} < 5.287 \text{ GeV}/c^2$. We then fit the ΔE distribution to extract the signal yield. In the rare cases where there is more than one candidate in an event (0.3% for $B^- \rightarrow D_{\text{sup}}K^-$ and 0.7% for $B^- \rightarrow D_{\text{sup}}\pi^-$), we select the best candidate on the basis of a χ^2 determined from the difference between the measured and nominal values of $M(K\pi)$ and M_{bc} .

The large background from the two jetlike $e^+e^- \rightarrow q\bar{q}$ ($q = u, d, s, c$) continuum processes is suppressed using variables that characterize the event topology. A Fisher discriminant [12] made up of modified Fox-Wolfram moments called the Super-Fox-Wolfram (SFW) [13] and $\cos\theta_B$, where θ_B is the angle of the B flight direction with respect to the beam axis in the c.m. system, are employed. These two independent variables, SFW and $\cos\theta_B$, are combined to form likelihoods for signal (\mathcal{L}_{sig}) and for continuum background ($\mathcal{L}_{\text{cont}}$); we then construct a likelihood ratio $\mathcal{R} = \mathcal{L}_{\text{sig}}/(\mathcal{L}_{\text{sig}} + \mathcal{L}_{\text{cont}})$. We optimize the \mathcal{R} requirement by maximizing $S/\sqrt{S+B}$, where S and B denote the expected numbers of signal and background events in the signal region, using Monte Carlo samples. To estimate S , we consider only the contribution from $B^- \rightarrow \bar{D}^0 K^-$ followed by $\bar{D}^0 \rightarrow K^+\pi^-$, where the value of r_B of Eq. (6) is taken to be 0.1. For $B^- \rightarrow D_{\text{sup}}K^-$ ($B^- \rightarrow D_{\text{sup}}\pi^-$) we require $\mathcal{R} > 0.90$

($\mathcal{R} > 0.74$), which retains 45% (70%) of the signal events and removes 99% (96%) of the continuum background. A similar \mathcal{R} requirement is obtained if the optimization uses S/\sqrt{B} instead of $S/\sqrt{S+B}$.

For $B^- \rightarrow D_{\text{sup}}K^-$, a possible background comes from $B^- \rightarrow D\pi^-$, $D \rightarrow K^+K^-$, which has the same final state and the same position of the ΔE peak as the signal. We veto events that satisfy $1.840 \text{ GeV}/c^2 < M(KK) < 1.890 \text{ GeV}/c^2$. After this veto, the estimated number of events that contribute to the signal yield is 0.22 ± 0.19 . The favored decay $B^- \rightarrow D_{\text{fav}}h^-$ can also produce a peaking background for the suppressed decay modes if both the kaon and the pion from the D_{fav} decay are misidentified and the particle assignments are interchanged. In order to remove this background, we veto events for which the invariant mass of the $K\pi$ pair is inside the $1.865 \text{ GeV}/c^2 \pm 0.020 \text{ GeV}/c^2$ window when the mass assignments are exchanged. After this requirement, we estimate that 0.17 ± 0.13 (6.0 ± 2.1) events contribute to the signal yield for $B^- \rightarrow D_{\text{sup}}K^-$ ($B^- \rightarrow D_{\text{sup}}\pi^-$).

The signal yields are extracted using extended unbinned maximum likelihood fits to the ΔE distributions. For the signal, we use a sum of two Gaussians, where the parameters are determined by a fit to $B^- \rightarrow D_{\text{fav}}\pi^-$. The same probability density function (PDF) is used for the signal peaks in all other modes; the validity of this assumption is verified by Monte Carlo studies.

Backgrounds from $B \rightarrow XK^-$ ($X \neq D_{\text{sup(fav)}}$), such as $B^- \rightarrow D^*K^-$, can populate the negative ΔE region of the $B^- \rightarrow D_{\text{sup(fav)}}K^-$ sample. The PDF for these backgrounds is obtained from the $B\bar{B}$ Monte Carlo samples, in which all known B and \bar{B} meson decays are allowed. Similarly, backgrounds from $B \rightarrow X\pi^-$ ($X \neq D_{\text{sup(fav)}}$), such as $B^- \rightarrow D^*\pi^-$ and $B^- \rightarrow D\rho^-$, can populate the negative ΔE region of the $B^- \rightarrow D_{\text{sup(fav)}}\pi^-$ sample, as well as the negative ΔE region of the $B^- \rightarrow D_{\text{sup(fav)}}K^-$ sample if the prompt pion is misidentified as a kaon. In the fit to $B^- \rightarrow D_{\text{sup(fav)}}\pi^-$ the PDF of these backgrounds is obtained from the $B\bar{B}$ Monte Carlo samples, while in the fit to $B^- \rightarrow D_{\text{sup(fav)}}K^-$ the PDF is obtained from data by assigning the kaon mass to the prompt pion track in the $B^- \rightarrow D_{\text{sup(fav)}}\pi^-$ sample. The good quality of the fit of the $B^- \rightarrow D_{\text{fav}}K^-$ data sample indicates the validity of this technique.

The feed-across from the $B^- \rightarrow D_{\text{sup(fav)}}\pi^-$ signal peak also appears in the fit to $B^- \rightarrow D_{\text{sup(fav)}}K^-$, where the prompt pion is misidentified as the kaon. The PDF is fixed from the fit to the $B^- \rightarrow D_{\text{fav}}\pi^-$ data sample where the kaon mass is assigned to the prompt pion track. The shift caused by the incorrect mass assignment makes the shape of the ΔE distribution asymmetric, and thus we model the misidentification background as a sum of two asymmetric Gaussians, for which the left and the right sides have different widths. In the fit to $B^- \rightarrow D_{\text{sup}}K^-$, we fix the yields for the contributions from the $B \rightarrow X\pi^-$ background and the feed-across from the $B^- \rightarrow D_{\text{sup}}\pi^-$ signal peak, using the measured yields

in the $B^- \rightarrow D_{\text{sup}}\pi^-$ sample scaled by the ratio of the $B^- \rightarrow D_{\text{fav}}\pi^-$ yields obtained in the $B^- \rightarrow D_{\text{fav}}K^-$ and $B^- \rightarrow D_{\text{fav}}\pi^-$ analyses.

The continuum background populates the entire ΔE region, for which we use a linear function. The fit results are shown in Fig. 2.

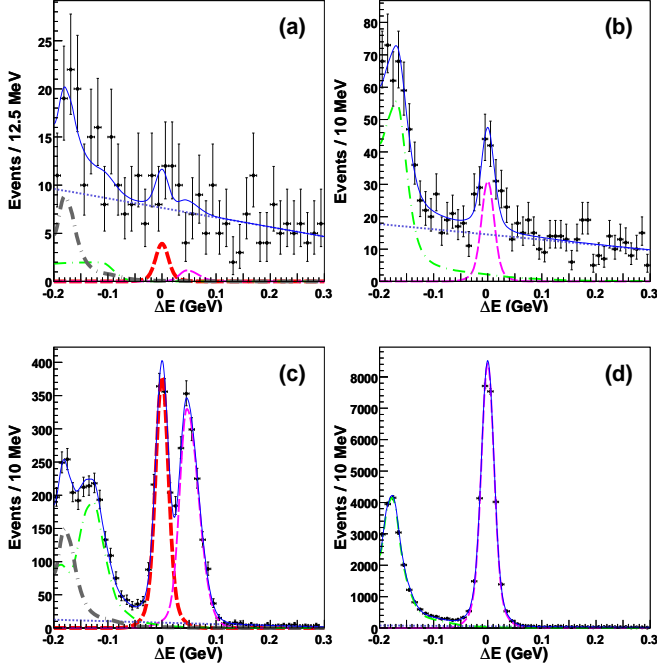


FIG. 2: ΔE distributions for (a) $B^- \rightarrow D_{\text{sup}}K^-$, (b) $B^- \rightarrow D_{\text{sup}}\pi^-$, (c) $B^- \rightarrow D_{\text{fav}}K^-$, and (d) $B^- \rightarrow D_{\text{fav}}\pi^-$. Charge conjugate decays are included. In these plots, $B^- \rightarrow DK^-$ components are shown by thicker dashed curves, and $B^- \rightarrow D\pi^-$ components are shown by thinner dashed curves. Backgrounds are shown by thicker dash-dotted curves (for $B \rightarrow XK^-$), thinner dash-dotted curves (for $B \rightarrow X\pi^-$), and dotted curves (for the continuum). The sum of all components is shown by the solid curves.

The charmless decay $B^- \rightarrow K^+K^-\pi^-$ ($B^- \rightarrow K^+\pi^-\pi^-$) can peak inside the signal region for $B^- \rightarrow D_{\text{sup}}K^-$ ($B^- \rightarrow D_{\text{sup}}\pi^-$). For this background, we fit the ΔE distribution of events in the D mass sideband, defined as $0.020 \text{ GeV}/c^2 < |M(K\pi) - 1.865 \text{ GeV}/c^2| < 0.080 \text{ GeV}/c^2$, and obtain an expected yield of -2.3 ± 2.4 (2.5 ± 4.5) events. We do not subtract this charmless contribution and instead include the uncertainties, $+2.4$ ($+4.5$), in the systematic error.

The signal yields (N_{Dh^-}) and the reconstruction efficiencies (ϵ_{Dh^-}) for the decays $B^- \rightarrow D_{\text{sup}}h^-$ and $B^- \rightarrow D_{\text{fav}}h^-$ are listed in Table I. From the results, we calculate ratios of branching fractions, defined as

$$R_{Dh} \equiv \frac{\mathcal{B}(B^- \rightarrow D_{\text{sup}}h^-)}{\mathcal{B}(B^- \rightarrow D_{\text{fav}}h^-)} = \frac{N_{D_{\text{sup}}h^-}/\epsilon_{D_{\text{sup}}h^-}}{N_{D_{\text{fav}}h^-}/\epsilon_{D_{\text{fav}}h^-}}. \quad (1)$$

We obtain

$$R_{DK} = [7.8^{+6.2}_{-5.7}(\text{stat})^{+2.0}_{-2.8}(\text{syst})] \times 10^{-3}, \quad (2)$$

$$R_{D\pi} = [3.40^{+0.55}_{-0.53}(\text{stat})^{+0.15}_{-0.22}(\text{syst})] \times 10^{-3}, \quad (3)$$

where the systematic errors (Table II) are subdivided as follows.

- (i) Fit: The uncertainties due to the PDFs of the $B^- \rightarrow D_{\text{sup}(\text{fav})}h^-$ decays and the $q\bar{q}$ background are obtained by varying the shape parameters by $\pm 1\sigma$. Those due to the PDFs and yields of the backgrounds from $B \rightarrow XK^-$ and $B \rightarrow X\pi^-$ are estimated by fitting the ΔE distribution in the region $-0.05 \text{ GeV} < \Delta E < 0.15 \text{ GeV}$ without including those contributions. The total fit error is the quadratic sum and 26% (3.1%) for R_{DK} ($R_{D\pi}$).
- (ii) Peaking backgrounds: The uncertainties due to the backgrounds which peak under the signal were described earlier, and the corresponding systematic error in R_{DK} ($R_{D\pi}$) is estimated to be $^{+2}_{-25}\%$ ($^{+2.2}_{-5.3}\%$). This uncertainty is asymmetric because the uncertainty of the charmless background is taken only for the negative side.
- (iii) Efficiency: Monte Carlo statistics and the uncertainties in the efficiencies of particle identification requirements dominate the systematic error in detection efficiency, which is estimated to be 2.7% (2.5%) for R_{DK} ($R_{D\pi}$).

The total systematic error is the sum in quadrature of the above uncertainties. The possible fit bias is checked using a large number of pseudoexperiments and found to be negligible.

The significances are estimated as $\sqrt{-2 \ln(\mathcal{L}_0/\mathcal{L}_{\text{max}})}$, where \mathcal{L}_{max} is the maximum likelihood and \mathcal{L}_0 is the likelihood when the signal yield is constrained to be zero. The distribution of the likelihood \mathcal{L} is obtained by convoluting the likelihood in the ΔE fit and an asymmetric Gaussian whose widths are the negative and positive systematic errors. The results are shown in Table I.

Since the signal for $B^- \rightarrow D_{\text{sup}}K^-$ is not significant, we set an upper limit at the 90% confidence level (C.L.), $R_{DK} < 1.8 \times 10^{-2}$. This limit, R_{DK}^{limit} , is calculated according to $\int_0^{R_{DK}^{\text{limit}}} \mathcal{L}(R_{DK}) dR_{DK} = 0.9 \times \int_0^\infty \mathcal{L}(R_{DK}) dR_{DK}$.

Using the values of R_{Dh} obtained above and the $B^- \rightarrow D_{\text{fav}}h^-$ branching fractions from Ref. [11], we determine the branching fractions for $B^- \rightarrow D_{\text{sup}}h^-$ from

$$\mathcal{B}(B^- \rightarrow D_{\text{sup}}h^-) = \mathcal{B}(B^- \rightarrow D_{\text{fav}}h^-) \times R_{Dh}. \quad (4)$$

The results are summarized in Table I. For the $B^- \rightarrow D_{\text{sup}}K^-$ branching fraction, we set an upper limit at the 90% C.L., $\mathcal{B}(B^- \rightarrow D_{\text{sup}}K^-) < 2.8 \times 10^{-7}$. Our branching fraction for $B^- \rightarrow D_{\text{sup}}\pi^-$ is consistent with the value expected from measured branching fractions for B and D decays [11].

TABLE I: Summary of the fit results. For the $B^- \rightarrow D_{\text{sup}}h^-$ signal yield, the contribution of peaking backgrounds has been subtracted. The first two errors on the measured branching fractions are statistical and systematic, respectively, and the third is due to the uncertainty in the $B^- \rightarrow D_{\text{fav}}h^-$ branching fraction used for normalization. The last column shows the partial rate asymmetries \mathcal{A}_{Dh} as explained in the text.

Mode	Efficiency (%)	Signal yield	Significance	Branching fraction [90% C.L. upper limit]	\mathcal{A}_{Dh}
$B^- \rightarrow D_{\text{sup}}K^-$	15.4 ± 0.3	$9.7^{+7.7}_{-7.0}$	1.3σ	$(1.2^{+1.0+0.3}_{-0.9-0.4} \pm 0.1) \times 10^{-7}$ [2.8×10^{-7}]	$-0.1^{+0.8}_{-1.0} \pm 0.4$
$B^- \rightarrow D_{\text{sup}}\pi^-$	23.1 ± 0.4	$93.8^{+15.2}_{-14.6}$	6.6σ	$(6.29^{+1.02+0.28}_{-0.98-0.41} \pm 0.24) \times 10^{-7}$	$-0.02^{+0.15}_{-0.16} \pm 0.04$
$B^- \rightarrow D_{\text{fav}}K^-$	15.1 ± 0.3	1220^{+41}_{-40}	\dots	\dots	\dots
$B^- \rightarrow D_{\text{fav}}\pi^-$	22.8 ± 0.4	27202^{+177}_{-176}	\dots	\dots	\dots

TABLE II: Summary of the systematic uncertainties for R_{DK} and \mathcal{A}_{Dh} .

Source	R_{DK}	$R_{D\pi}$	\mathcal{A}_{DK}	$\mathcal{A}_{D\pi}$
Fit	$\pm 26\%$	$\pm 3.1\%$	± 0.40	± 0.04
Peaking backgrounds	$+2\%$ -25%	$+2.2\%$ -5.3%	\dots	\dots
Efficiency	$\pm 2.7\%$	$\pm 2.5\%$	\dots	\dots
Detector asymmetry	\dots	\dots	± 0.01	± 0.01

The ratio R_{DK} is related to ϕ_3 by

$$R_{DK} = r_B^2 + r_D^2 + 2r_B r_D \cos \phi_3 \cos \delta \quad (5)$$

where [14]

$$r_B \equiv \left| \frac{A(B^- \rightarrow \bar{D}^0 K^-)}{A(B^- \rightarrow D^0 K^-)} \right|, \quad \delta \equiv \delta_B + \delta_D, \quad (6)$$

$$r_D \equiv \left| \frac{A(D^0 \rightarrow K^+ \pi^-)}{A(D^0 \rightarrow K^- \pi^+)} \right| = 0.0578 \pm 0.0008, \quad (7)$$

and δ_B and δ_D are the strong phase differences between the two B and D decay amplitudes, respectively. Using the above result, we obtain a conservative upper limit on r_B as follows. For a given R_{DK} and in the relevant parameter ranges, r_B is the largest when $\cos \phi_3 \cos \delta = -1$ and r_D is maximal. Thus, we take $\cos \phi_3 \cos \delta = -1$ and a $+2\sigma$ shift in r_D , and obtain $r_B < 0.19$ which corresponds to the 90% upper limit on R_{DK} .

We also measure the partial rate asymmetry \mathcal{A}_{Dh} in the $B^\mp \rightarrow D_{\text{sup}}h^\mp$ decays,

$$\mathcal{A}_{Dh} \equiv \frac{\mathcal{B}(B^- \rightarrow D_{\text{sup}}h^-) - \mathcal{B}(B^+ \rightarrow D_{\text{sup}}h^+)}{\mathcal{B}(B^- \rightarrow D_{\text{sup}}h^-) + \mathcal{B}(B^+ \rightarrow D_{\text{sup}}h^+)}, \quad (8)$$

by fitting the B^- and B^+ candidates with the asymmetry as one of the fitting parameters. The fit results are shown in Fig. 3 and included in Table I. We obtain

$$\mathcal{A}_{D\pi} = -0.02^{+0.15}_{-0.16}(\text{stat}) \pm 0.04(\text{syst}) \quad (9)$$

and no significant constraint on \mathcal{A}_{DK} . The systematic errors (Table II) are dominated by the uncertainties due

to the fits. Possible bias due to charge asymmetry of the detector is estimated using the $B^- \rightarrow D_{\text{fav}}\pi^-$ control sample for which the expected asymmetry is small. The peaking backgrounds are subtracted assuming no CP asymmetries. An assumption of 30% CP asymmetry in the peaking background would lead to a shift of 0.02 in $\mathcal{A}_{D\pi}$.

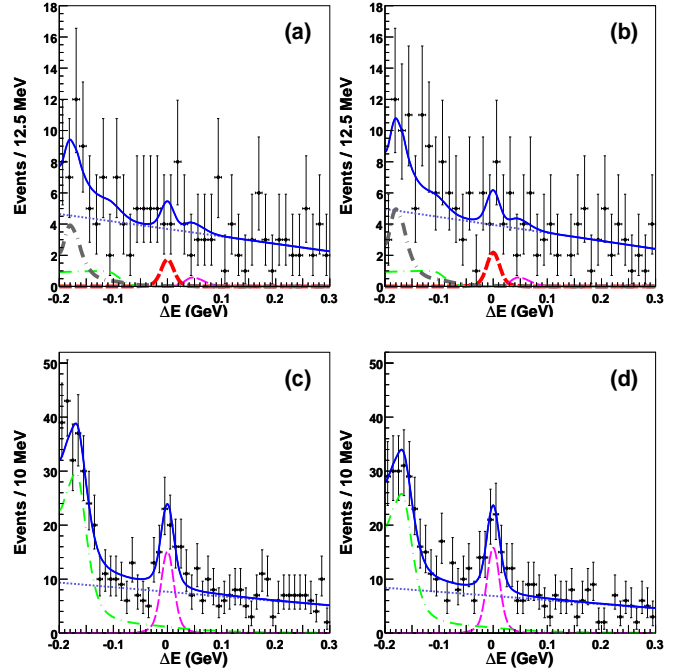


FIG. 3: ΔE distributions for (a) $B^- \rightarrow D_{\text{sup}}K^-$, (b) $B^+ \rightarrow D_{\text{sup}}K^+$, (c) $B^- \rightarrow D_{\text{sup}}\pi^-$, and (d) $B^+ \rightarrow D_{\text{sup}}\pi^+$. The curves show the $B^\mp \rightarrow D_{\text{sup}}K^\mp$ component (thicker dashed curves), the $B^\mp \rightarrow D_{\text{sup}}\pi^\mp$ component (thinner dashed curves), and the background components (thicker dash-dotted curves for $B \rightarrow XK^\mp$, thinner dash-dotted curves for $B \rightarrow X\pi^\mp$, and dotted curves for the continuum), as well as the overall fit (solid curves).

We also report the ratio

$$\frac{\mathcal{B}(B^- \rightarrow D^0 K^-)}{\mathcal{B}(B^- \rightarrow D^0 \pi^-)} = \frac{N_{D_{\text{fav}} K^-} / \epsilon_{D_{\text{fav}} K^-}}{N_{D_{\text{fav}} \pi^-} / \epsilon_{D_{\text{fav}} \pi^-}} \quad (10)$$

to be $[6.77 \pm 0.23(\text{stat}) \pm 0.30(\text{syst})] \times 10^{-2}$ from the fit to $B^- \rightarrow D_{\text{fav}} K^-$ and $B^- \rightarrow D_{\text{fav}} \pi^-$, which is about 3σ lower than the current world average [11]. The systematic error is due to the uncertainties in the yield extractions (3.1%) and uncertainties in efficiency estimations (1.9%). The latter is dominated by the uncertainty in particle identification efficiency for prompt hadrons.

In summary, using 657×10^6 $B\bar{B}$ pairs collected with the Belle detector, we report studies of the suppressed decay $B^- \rightarrow D_{\text{sup}} h^-$ ($h = K, \pi$). No significant signal is observed for $B^- \rightarrow D_{\text{sup}} K^-$ and we set a 90% C.L. upper limit on the ratio of B decay amplitudes, $r_B < 0.19$. This result is consistent with the measurement of

r_B in the Dalitz plot analysis of the decay $B^- \rightarrow DK^-$, $D \rightarrow K_S^0 \pi^+ \pi^-$ [15, 16]. For $B^- \rightarrow D_{\text{sup}} \pi^-$, we observe a signal with 6.6σ significance. We also report the charge asymmetry for $B^\pm \rightarrow D_{\text{sup}} \pi^\mp$ and the ratio $\mathcal{B}(B^- \rightarrow D^0 K^-) / \mathcal{B}(B^- \rightarrow D^0 \pi^-)$. These results improve and supersede our previous results [6, 17].

We thank the KEKB group for excellent operation of the accelerator, the KEK cryogenics group for efficient solenoid operations, and the KEK computer group and the NII for valuable computing and Super-SINET network support. We acknowledge support from MEXT and JSPS (Japan); ARC and DEST (Australia); NSFC (China); DST (India); MOEHRD, KOSEF and KRF (Korea); KBN (Poland); MES and RFAAE (Russia); ARRS (Slovenia); SNSF (Switzerland); NSC and MOE (Taiwan); and DOE (USA).

-
- [1] N. Cabibbo, Phys. Rev. Lett. **10**, 531 (1963).
[2] M. Kobayashi and T. Maskawa, Prog. Theor. Phys. **49**, 652 (1973).
[3] I. I. Bigi and A. I. Sanda, Phys. Lett. B **211**, 213 (1988).
[4] M. Gronau and D. London, Phys. Lett. B **253**, 483 (1991); M. Gronau and D. Wyler, Phys. Lett. B **265**, 172 (1991).
[5] D. Atwood, I. Dunietz, and A. Soni, Phys. Rev. Lett. **78**, 3257 (1997); Phys. Rev. D **63**, 036005 (2001).
[6] Belle Collaboration, M. Saigo *et al.*, Phys. Rev. Lett. **94**, 091601 (2005).
[7] BaBar Collaboration, B. Aubert *et al.*, Phys. Rev. Lett. **93**, 131804 (2004); Phys. Rev. D **72**, 032004 (2005).
[8] S. Kurokawa and E. Kikutani, Nucl. Instr. and Meth. A **499**, 1 (2003), and other papers included in this volume.
[9] Belle Collaboration, A. Abashian *et al.*, Nucl. Instr. and Meth. A **479**, 117 (2002).
[10] Belle SVD2 Group, Z. Natkaniec *et al.*, Nucl. Instr. and Meth. A **560**, 1 (2006).
[11] Particle Data Group, W.-M. Yao *et al.*, 2007 partial update for the 2008 edition at <http://pdg.lbl.gov>.
[12] R. A. Fisher, Ann. Eugenics **7**, 179 (1936).
[13] The Fox-Wolfram moments were introduced in G. C. Fox and S. Wolfram, Phys. Rev. Lett. **41**, 1581 (1978). The modified moments used in this paper are described in Belle Collaboration, S. H. Lee *et al.*, Phys. Rev. Lett. **91**, 261801 (2003).
[14] HFAG, online update for Charm 2007 at <http://www.slac.stanford.edu/xorg/hfag/charm>.
[15] Belle Collaboration, A. Poluektov *et al.*, Phys. Rev. D **73**, 112009 (2006).
[16] BaBar Collaboration, B. Aubert *et al.*, Phys. Rev. Lett. **95**, 121802 (2005).
[17] Belle Collaboration, S. K. Swain *et al.*, Phys. Rev. D **68**, 051101 (2003).